Future changes, or lack thereof, in the temporal variability of the combined wind-plus-solar power production in Europe

S. Jerez, I. Tobin, M. Turco, P. Jiménez-Guerrero, R. Vautard, J.P. Montávez

Renewable Energy 139 (2019) 251–260

Contents lists available at ScienceDirect

Renewable Energy

journal homepage: www.elsevier.com/locate/renene

Future changes, or lack thereof, in the temporal variability of the combined wind-plus-solar power production in Europe

S. Jerez [a, *], I. Tobin [b], M. Turco [c], P. Jiménez-Guerrero [a], R. Vautard [b], J.P. Montávez [a]

[a] Regional Atmospheric Modeling (MAR) Group, Department of Physics, University of Murcia, 30100 Murcia, Spain
[b] Laboratoire des Sciences du Climat et de l'Environnement, 91191 Gif sur Yvette, France
[c] Earth Science Department, Barcelona Supercomputing Center (BSC), 08034 Barcelona, Spain

ARTICLE INFO

Article history:
Received 30 July 2018
Received in revised form
10 January 2019
Accepted 12 February 2019
Available online 16 February 2019

Keywords:
Wind power
Solar photovoltaic power
Climate change
Supply variability

ABSTRACT

Here we present the first assessment of climate change impacts on the temporal variability of the joint production of wind and solar photovoltaic (PV) power across Europe. For that we adopted regional and continental perspectives (assuming a single European electricity grid), considered several temporal frequencies (from daily to annual), used state-of-the-art regional climate projections together with a climate-production model, and assumed a future massive deployment of wind and PV power installations. Results support that the spatio-temporal complementarity between the wind and solar resources helps to minimize the temporal variability of the combined production under both present (1971–2000) and future (2070–2099) climate conditions similarly. Thus the projected changes are overall negligible (well below ±5%). However, an additional assessment of theoretical upper/bottom bounds for these changes indicated significant potential increases in the stability of the joint production ranging from 5 to 25% across regions, 15% at the continental scale. This would be subordinated to the feasibility of reaching, with the future deployment strategies, individual wind and PV power production series with a perfect temporal anticorrelation. These results may encourage stakeholders to take holistically optimized decisions.

1. Introduction

The transition to renewables plays a key role in the climate change mitigation strategies [1], as well as in the response to the challenges of fossil fuel depletion [2,3] and air quality upkeep and improvement [4]. Besides, national energy independence targets require increased shares of electricity production from the free, local and clean renewable energy resources, such as wind and solar [5,6]. However, a high penetration of wind and solar power in the grid, such as proposed for future energy mix scenarios in Europe [7], increases the dependence of the power supply on weather and climate conditions. This dependence induces variability and, therefore, the need for backup and storage energy systems to prevent blackouts [8,9]. This calls for holistic deployment plans aimed at exploiting the spatio-temporal complementarity of the resources [10–17] and thereby minimizing the uncontrollable variability of the renewable supply. On the other hand, the long-term projected changes in near-surface wind speed and cloudiness directly impact the amount of energy produced by wind and solar photovoltaic (PV) power farms respectively [18–23]. Therefore, the vulnerability of the renewable production to climate change could pose an additional issue, not only in terms of changes in the mean production, but also in terms of changes in the temporal stability of the production.

In terms of mean production, in Europe, previous works have shown that the climate change impact on PV and wind power is limited but overall negative. Projected reductions are in the range 0–10%, being, roughly, more pronounced northward for PV and southward for wind power [20,22–24]. Still these depletions would be smaller than those estimated for the two other main sub-sectors of the electricity market, namely hydro and thermo-electric [25]. In particular, the projected change in thermo-electric power generation using river water for cooling involves reductions as large as three times higher than for PV and wind power due to future river water scarcity and warming. Hence, it seems doubly beneficial to increase the wind and PV power share in combination with reducing thermo-electric power (primarily fossil-fuel based power) in the European energy mix, which, in turn, could increase the

* Corresponding author.
E-mail address: sonia.jerez@um.es (S. Jerez).

https://doi.org/10.1016/j.renene.2019.02.060

energy mix vulnerability to climate change in terms of the variability of the supply.

The impact of climate change on the temporal variability of PV and wind power production, individually, over Europe, has been assessed in Jerez et al. [20] and Tobin et al. [23] respectively. For both powers, projected changes are essentially small (less than 10%) on either high (daily), medium (monthly) or low (yearly) time frequencies. As for the mean production, worse signals (higher variability in the future) were found northward for PV and southward for wind power. Either way, the whole issue, i.e. the behavior of the PV-plus-wind power generation in terms of its temporal variability under changed climate conditions, is more than the sum of its parts (shaped by the temporal co-variability between PV and wind power production series) and still remains unveiled.

The main goal of this study is to shed light on the climate change impacts on the temporal variability of the combined electricity production from wind and solar PV power over Europe. This is done both at regional and continental scales (i.e. for the ideal case of a single European electricity grid, as encouraged from the European Commission; https://cordis.europa.eu/programme/rcn/664349_en.html) using a consistent approach based on common six-member ensemble of state-of-the-art regional climate model projections and considering future massive deployments of wind and PV power installations aimed at reaching the 80% renewable energy supply goal set by the European Climate Foundation [7]. Impacts are further assessed under the ideal assumption of perfectly anti-correlated PV and wind power production series with the aim of providing, along with the actual projected changes in the stability of the joint PV-plus-wind power production, upper bounds for potential achievements based on a smart optimization of the spatio-temporal complementarity between the PV and wind powers in their response to the projected climate change.

2. Data and methods

2.1. Climate data

Six Euro-Cordex (https://www.euro-cordex.net/) simulations, spanning historical (1971–2000) and scenario (2070–2099) periods, were used (Table 1). The latter were developed under the most challenging Representative Concentration Pathway RCP8.5 [26]. These simulations were chosen based on their previous and coincident use in the works by Tobin et al. [23] and Jerez et al. [20]. As for these previous works, 3-hourly time series of 10-m wind speed (W), surface downward solar radiation (R) and near surface air temperature (T) were retrieved from the climate simulations and used for the estimation of wind and PV power production series.

2.2. PV and wind power deployment plans

Estimations of power production require the knowledge of the penetration level of the variable renewables in the energy system. We considered the mixes defined by the European Climate Foundation [7] in its ambitious 80% Renewable Energy Supply (RES) low-carbon pathway. As part of the climate change mitigation strategies, the 80% RES pathway establishes high PV and wind power shares in the European energy mix for the year 2050 (specified per regions; see Table 2) contributing to about 50% of the total power supply (1/3 from PV, 2/3 from wind power installations).

2.3. Modeling power production

Wind and PV power production series were estimated at the grid point level (using the Euro-Cordex compliant domain) and thereof aggregated per regions. At the grid point level, they were obtained by combining weather-production models (driven by the simulated 3-hourly W, R and T series) and the spatial disaggregation of wind and PV power installations provided by the CLIMIX model [27] from the regional totals of installed capacity listed in Table 2, exactly as in Tobin et al. [23] and Jerez et al. [20]. The obtained 3-hourly regional production series were then aggregated at the daily time-scale. The resulting PV and wind power series were finally added to construct the PV-plus-wind power production series analyzed here.

Table 2
Spatial coverage of each region and amount of wind and PV power total capacity installed (in GW) as proposed by the European Climate Foundation in the 80% RES pathway for 2050 [7]].

Region	Spatial coverage (nations)	Wind	PV
Nordic	Denmark, Finland, Norway, Sweden	76	23
UK-Ireland	Ireland, UK	106	46
Benelux-Germany	Belgium, Germany, The Netherlands	99	114
Iberia	Portugal, Spain	43	180
Poland-Baltic	Estonia, Latvia, Lithuania, Poland	21	40
Central Europe	Austria, Czech Rep., Slovakia, Slovenia, Switzerland	16	137
South East Europe	Bulgaria, Cyprus, Greece, Hungary, Romania	5	76
Italy-Malta	Italy, Malta	22	121
France	France	51	133
EUROPE	All the above	439	870

Table 1
List of climate simulations used in this study. First column provides its short identifier, second the name of the institution where it was carried out, third the RCM and fourth the GCM run driving the RCM in each case. For further details on the models and their setups, see Tobin et al. [23] and Jerez et al. [20]. Data are available upon contact the corresponding author.

Exp. ID	Institution	RCM	GCM driving run
DMI	Danish Meteorological Institute	HIRHAM5	EC-EARTH (r3i1p1) run at the Irish Centre for High-End Computing (ICHEC)
IPSL	Institute Pierre Simon Laplace - Institut National de l'Environment Industriel et des Risques	WRF3.3.1	IPSL-CM5A-MR (r1i1p1) run at the Institute Pierre Simon Laplace (IPSL)
KNMI	Royal Netherlands Meteorological Institute	RACMO2.2	EC-EARTH (r1i1p1) run at the Irish Centre for High-End Computing (ICHEC)
SMHI-CNRM	Swedish Meteorological and Hydrological Institute	RAC4	CNRM-CM5 (r1i1p1) run at the National Centre for Meteorological Research (CNRM)
SMHI-ICHEC	Swedish Meteorological and Hydrological Institute	RAC4	EC-EARTH (r12i1p1) run at the Irish Centre for High-End Computing (ICHEC)
SMHI-MOHC	Swedish Meteorological and Hydrological Institute	RAC4	HadGEM2-ES (r1i1p1) run at the Met Office Hadley Centre (MOHC)

2.4. Decomposition of the temporal variability of the daily production series

The temporal variability of the daily production series is decomposed at various temporal frequencies as follows. Let d be the daily data, m their monthly means (twelve values per year), and y their annual means. Then:

$$d = y + m' + d' \tag{1}$$

where m' is the monthly anomaly relative to the corresponding annual mean ($m' = m\text{-}y$) and d' is the daily anomaly relative to the corresponding monthly mean ($d' = d\text{-}m$). m' and d' can be further developed as:

$$m' = \overline{m'} + \left(m' - \overline{m'}\right) \tag{2}$$

$$d' = \overline{d'} + \left(d' - \overline{d'}\right) \tag{3}$$

where $\overline{m'}$ is the multi-year monthly mean of m' and $\overline{d'}$ is the multi-year daily mean of d'.

Hence, Eq. (1) includes the following terms:

$$d = y + \overline{m'} + \left(m' - \overline{m'}\right) + \overline{d'} + \left(d' - \overline{d'}\right) \tag{4}$$

We used the standard deviation (S) of each term to account for their temporal variability, expressed in percentage with respect to a normalizing factor given by the mean value of the daily series in order to obtain comparable values among all regions. This way S_d represents the variability of the whole daily series (WDS); S_y represents the year-to-year (Y2Y) or inter-annual variability of the WDS; $S_{\overline{m'}}$ represents the width of the annual cycle after removing the inter-annual variability, hence the monthly intra-annual variability (MIA); $S_{m'-\overline{m'}}$ represents the monthly noise, the monthly variations with respect to the annual cycle, thus the month-to-month variability (M2M); $S_{\overline{d'}}$ represents the variations of the daily anomalies after removing the corresponding monthly means of the series, hence the daily intra-monthly variability (DIM); and $S_{d'-\overline{d'}}$ represents the residual daily noise after removing the cyclicity signals at lower frequencies (monthly and yearly), thus the day-to-day variability (D2D). We did not include the DIM term in this assessment because, in the case of the PV power, $\overline{d'}$ series are step functions dominated by Earth orbital factors.

2.5. Robustness criteria for the ensemble mean signals

The statistical significance of the differences between present and future values was evaluated using the Student's t-test, after the convenient F-transformation applied to the standard deviations of the series and Fisher's z-transformation applied to the temporal correlations, imposing $p < 0.05$. The ensemble mean projected signals are then considered robust when at least 3 individual signals (out of 6, 50% of experiments) are significant and agree in the sign, and any significant signal has opposite sign. If there are at least two significant signals with different signs, the ensemble mean signal is considered uncertain. If there are not significant signals disagreeing in the sign, but there are less than 3 significant signals with the same sign, the ensemble mean signal is considered negligible. This criteria follows Jerez et al. [20].

2.6. Quantification of the role of the PV and wind power (anti) correlation on the variability of the joint PV-plus-wind power production

As long as the wind and the solar resources behaves complementary, with the PV and wind power (WP) production series being anticorrelated in time, the standard deviation of the series of PV-plus-wind power joint production is reduced as compared to the results from uncorrelated or positively correlated individual production series. This can be easily recognized from the following formulations relating ρ (the Pearson correlation coefficient between two series), Cov (the covariance of the two series) and S:

$$\rho = \frac{Cov(PV, WP)}{S_{PV} S_{WP}} \tag{5}$$

$$S^2_{PV+WP} = S^2_{PV} + S^2_{WP} + 2Cov(PV, WP) = S^2_{PV} + S^2_{WP} + 2\rho S_{PV} S_{WP} \tag{6}$$

Since ρ could range between −1 and 1, Eq. (6) implies:

$$\sqrt{S^2_{PV} + S^2_{WP} - 2S_{PV}S_{WP}} \le S_{PV+WP} \le \sqrt{S^2_{PV} + S^2_{WP} + 2S_{PV}S_{WP}} \tag{7}$$

Eq. (7) thus establishes bottom and upper bounds for the standard deviation of the joint PV-plus-wind power production series as ρ varies from −1 to 1. Taking S_{PV+WP} for $\rho = 0$ as reference value ($S_{REF} = \sqrt{S^2_{PV} + S^2_{Wp}}$), the gains or losses in the stability of the combined production with respect to the reference state as ρ takes negative or positive values, respectively, thus fulfill:

$$S_{REF} - \sqrt{S^2_{PV} + S^2_{WP} + 2S_{PV}S_{WP}} \le S_{REF} - S_{PV+WP} \le S_{REF} - \sqrt{S^2_{PV} + S^2_{WP} - 2S_{PV}S_{WP}} \tag{8}$$

where the central term represents the gain or loss of stability (the more positive, the greater the gain) for actual values of ρ in a given period. We computed the terms in Eq. (8) in percentage with respect to the mean production, as indicated in Section 2.4, for comparative purposes.

Applying Eq. (6), the projected changes in the standard deviation of the series can be written as:

$$\begin{aligned} \Delta S_{PV+WP} &= S'_{PV+WP} - S_{PV+WP} \\ &= \sqrt{S'^2_{PV} + S'^2_{WP} + 2\rho' S'_{PV} S'_{WP}} \\ &\quad - \sqrt{S^2_{PV} + S^2_{WP} + S^2_{WP} + 2\rho S_{PV} S_{WP}} \equiv F\left(\rho'\right) \end{aligned} \tag{9}$$

where the values in future periods are denoted with prime symbols. Here S_{PV+WP} and S'_{PV+WP} will be also computed in percentage with respect to the mean production values of the respective periods.

In order to quantify the isolated effect of the changes in ρ, we considered ΔS_{PV+WP} (Eq. (9)) as a function of ρ' (F(ρ')). Taking into account that ρ′ could range between −1 and 1, the upper and bottom bounds for the changes in the standard deviation of the joint PV-plus-wind power production series due to the changes in the temporal correlation between the individual PV and wind power production series are given by F(1) and F(-1) respectively, thus:

$$F(-1) \leq \Delta S_{PV+WP} \leq F(1) \quad (10)$$

From where, taking as reference value for ρ′ its value in the historical period (namely, $\rho'_{REF} = \rho$) to account for the future changes in S_{PV+WP} related to the future changes in ρ, we have:

$$F\left(\rho'_{REF}\right) - F(1) \leq F\left(\rho'_{REF}\right) - \Delta S_{PV+WP} \leq F\left(\rho'_{REF}\right) - F(-1) \quad (11)$$

Eq. (11) thus permits to assess the effect of changes in the temporal correlation between the PV and the wind power production series on the projected changes in the temporal variability of the joint PV-plus-wind production series, as well its upper and bottom limits.

3. Results

3.1. Unraveling the impact of climate change on PV-plus-wind power variability

Fig. 1 shows the climatologies under present and future conditions of the mean and the temporal variability of the whole daily production series considering only the PV power output (yellow), only wind (blue), or the sum of both (PV-plus-wind; green), along with the projected changes in these magnitudes to the end of the century. Climatologies and projected changes for the temporal variability of the series at the time frequencies described in Section 2.4 (Y2Y, MIA, M2M and D2D) are analogously displayed in Fig. 2.

Changes in mean production (Fig. 1b) are very similar to those reported in previous works [20,23,25], despite the particular sub-ensemble of climate simulations considered here. Changes in mean PV-plus-wind power production are negative and robust for all regions, but limited to below 5% according to the ensemble mean signals. In the Nordic region, where climate change impact on mean PV power production is highest (~10%), the high share of wind power (see Table 2) reduces the impact on the total PV-plus-wind mean production (~2%), as wind power is less affected. On the contrary, in the Iberian region, where the impact on wind power is highest (>5%), the high share of PV power (see Table 2) reduces the impact on the total PV-plus-wind mean production (<2%), as PV power is less affected. At the continental scale, projections for either PV, wind or PV-plus-wind mean power production involve reductions of a few (2–3) percentage points.

The temporal variability (normalized standard deviation) of the whole daily PV-plus-wind power production series is lower than for the PV or wind power series individually (Fig. 1c). This holds for all European regions under both present and future climate

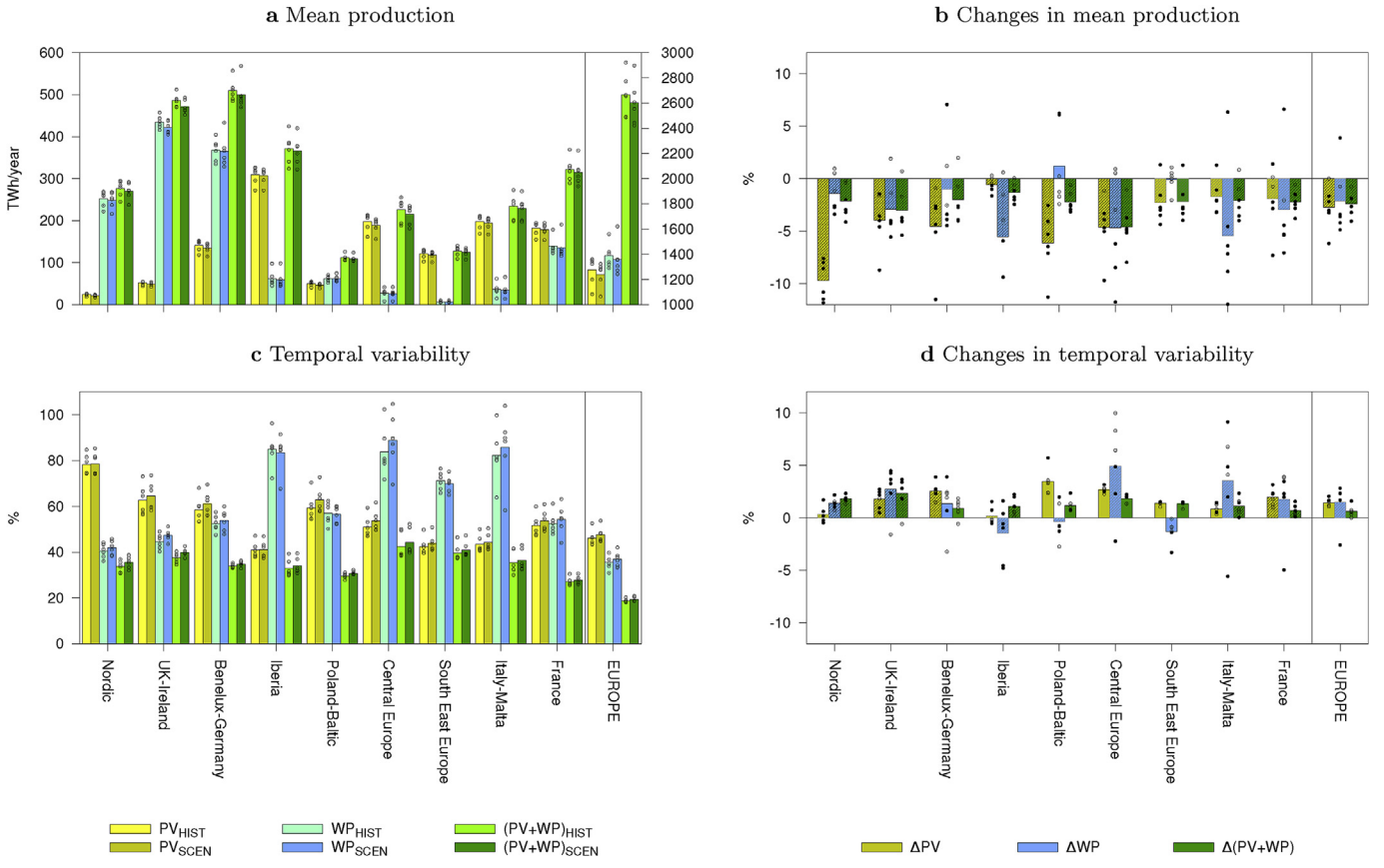

Fig. 1. *Climatologies and changes in the mean PV-plus-wind power production and its temporal variability.* Climatologies (left column; light colors correspond to historical values, period 1971–2000; dark colors correspond to scenario values, period 2070 2099; PV, wind and PV-plus-wind power production in yellow, blue and green respectively) and futures changes (right column) for the mean and the temporal variability of the daily production series modeled for each European region (see Methods for the modeling approach). Mean production is expressed in TWh/year (values for the whole Europe are referred to the right y-axis) and its changes as future minus present values, given in % respect to present values. Temporal variability is computed as the normalized standard deviation of the whole daily series (i.e. standard deviation divided by the mean value of the series) and expressed in % respect to the mean value of the series. Its changes are just given as future minus present values (units are % but they do not represent variations in relative terms as in the case of mean production changes). Color bars represent ensemble mean values. Symbols correspond to each single model/experiment. In the right panels, black/gray-striped colored bars denote robust/uncertain ensemble mean change signals, empty colored bars denote negligible ensemble mean change signals, and solid/empty symbols denote significant/non-significant individual change signals (see Methods for the followed criteria).

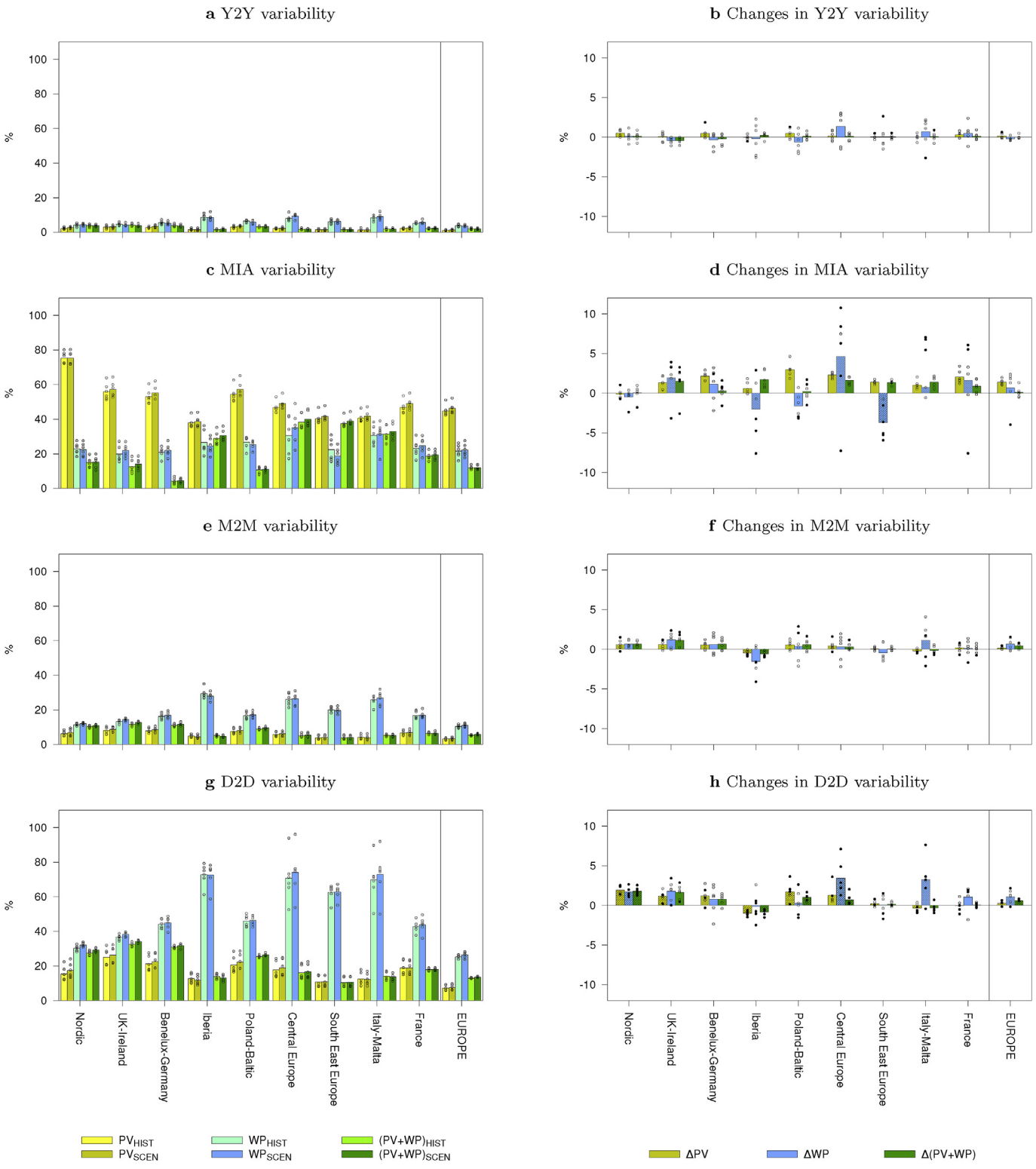

Fig. 2. *Climatologies and changes in the temporal variability of the PV-plus-wind power production at various frequencies.* As Fig. 1c and d but for the year-to-year (Y2Y; a,b), monthly intra-annual (MIA; c,d), month-to-month (M2M; e,f) and day-to-day (D2D; g,h) variability of the production series (see definitions in Methods).

conditions, revealing a certain degree of temporal complementarity between both renewable energies whatever the climate scenario is. At the continental scale, for instance, the variability of the PV power production represents about 50% of the mean PV power generation, about 30% for the wind. However, the variability of the PV-plus-wind power production represents "only" a 20% of the total mean production. To the future, S_{PV+WP} is projected to undergo robust changes, mostly increases, while limited to a few percents all over Europe, with the ensemble mean signals well below 5% (Fig. 1d). Interestingly, in the regions of Benelux-Germany, Central Europe and France, also at the continental scale, the climate change signals for S_{PV+WP} are lower than for the individual PV and wind power

series, may indicating a certain increase in the complementarity between the WP and PV series in their response to climate change (i.e. $\rho'<\rho$, Eq. (9)). By contrast, the projected increase in the variability of the PV-plus-wind production series exceeds the projections made for the individual series of wind or PV production in the Nordic and Iberian regions. In the rest of regions (UK-Ireland, Poland-Baltic, South East Europe and Italy-Malta regions), the climate change signals for S_{PV+WP} are in between those for S_{WP} and those for S_{PV}.

Among the set of temporal frequencies analyzed here, the highest values of S_{PV+WP} arise for the MIA and D2D terms (left column panels in Fig. 2; see also first column panels of Fig. 4), while also complementarity (i.e. $S_{PV+WP} < S_{PV}$ and $S_{PV+WP} < S_{WP}$) outstands the most for these two terms, similarly in both the historical and the scenario period. In the northernmost regions, and also at the continental scale, complementarity works mostly at the MIA time frequency, indicating that the annual cycles of PV and wind power production are somehow inverted (the anticorrelation values at the MIA time-scale are indeed high, Fig. 3a,c). The higher share of wind power than of PV power in northern regions (see Table 2) also helps to reduce the MIA variability of the PV-plus-wind power series as compared to the individual power production series, as the MIA variability is lower for the wind power (Fig. 2c). Over central and southern Europe, complementarity outstands the most at the D2D time frequency, partly because of the anticorrelation between the two powers (although the anticorrelation values at the D2D time-scale are not very high, Fig. 3a,c), but mostly due to the higher share of PV power than of wind power (see Table 2), as the D2D variability is lower for the PV power (Fig. 2g).

In terms of changes (right column panels in Fig. 2) the largest signals arise precisely at these two time-scales (MIA and D2D), being generally positive while small (<5%). Consequently, most of the ensemble mean signals are either negligible or uncertain (see also second column panels of Fig. 4). Still, it can be appreciated that the hypothesis of complementarity between PV and wind power in their response to climate change (i.e. $\Delta S_{PV+WP}<\Delta S_{PV}$ and $\Delta S_{PV+WP}<\Delta S_{WP}$) holds, at least partially (i.e. ΔS_{PV+WP} at least in between ΔS_{PV} and ΔS_{WP}), in almost all regions and for all the terms (with the exceptions of the changes projected in the MIA variability for Iberia and in the M2M variability for the Nordic region). This is particularly appreciable at the continental scale. It is also clear from this analysis that the reduced ΔS_{PV+WP} as compared to ΔS_{PV} and ΔS_{WP} identified above for the WDS in the regions of Benelux-Germany, Central Europe and France (Fig. 1d) responds predominantly to the reduced impact on the MIA variability when the PV-plus-wind combined approach is considered (Fig. 2d). Notably, in Central Europe, the projected changes in the D2D variability are also lower for the combined series as compared to the signals for PV and wind power (Fig. 2h).

3.2. Actual and potential effect of (anti)correlation between PV and wind power series

PV and wind power production series are anticorrelated in time, which holds both in the historical and the scenario periods similarly at any time frequency (the only exceptions appear in South East Europe for the Y2Y and M2M terms and in the Italy-Malta region for the Y2Y term; Fig. 3a,c). This helps to reduce the temporal variability of the joint PV-plus-wind power series (Eq. (6)). Such anticorrelation outstands the most at the MIA time frequency, with ρ close to -1 in most regions and scenarios. As a result, the standard deviation of the MIA PV-plus-wind power production series is notably lower than it would be in the case of non-correlated individual production series (the reference state taken to quantify benefits derived from the PV and wind power complementarity, as described in Section 2.6). The gain is above 15% in the regions of Benelux-Germany and Poland-Baltic; 12% at the continental scale (Fig. 3b,d). At the D2D time frequency, gains are a bit milder but still notable, e.g. ~10% at the continental scale. However, the upper theoretical limits for the gain in stability are still far. For the whole daily series, it could be up to almost 40% regionally, ~25% at the continental scale, if totally anticorrelated individual production series could be achieved (see range-bars in Fig. 3b,d).

In terms of changes, it has been already anticipated that the correlation between the PV and the wind power production series (ρ) is expected to remain basically as it is (Fig. 3e). This, together with the small changes projected for both S_{PV} and S_{WP}, explains the small changes projected for ΔS_{PV+WP} (Fig. 1d and right panels in Fig. 2). As the effect of the projected changes in ρ on the projected changes in S_{PV+WP} is thus quite limited (Fig. 3f), the interest here is to evaluate how it could be given the range of variation allowed for the correlation. Results show that negative change signals in ρ would allow to enlarge the stability of the total production daily series by, as much, 10–20% in several regions (e.g. Benelux-Germany, Iberia, Poland-Baltic, France) and at the European level (see range-bars in Fig. 3f). Benefits would come mostly from a larger stability at the D2D time frequency (up to 10% in several regions, e.g. Iberia, Poland-Baltic, Central Europe, Italy-Malta and France), since ρ is already close to the ideal -1 value at the MIA time frequency in both present and future scenarios, and the two other terms, Y2Y and M2M, have actually revealed as the least important ones (Section 3.1).

3.3. Synthesis analysis

A synthesis analysis is presented in Fig. 4. First column depicts S_{PV+WP} in the historical period, second column the actual ensemble mean projected changes in S_{PV+WP}, and third column the potential ensemble mean projected changes in S_{PV+WP} for an ideal value of $\rho = -1$ in the future period (i.e. F(-1) according to the notation of Section 2.6, Eq. (9)). Gray and black colors mask the negligible and uncertain signals, respectively.

The variability (standard deviation) of the PV-plus-wind power production series in the historical period ranges from 20 to 40% of the mean production across regions (Fig. 4a). At the European scale, it drops to a bit below 20%, which is likely due to the higher wind-and-solar spatio-temporal complementarity potential over wide regions. The highest contribution to the variability of the whole daily series come from the MIA and the D2D terms, the former being highest in southern regions (Fig. 4g), the latter in northern ones (Fig. 4m).

Projected changes are well bellow 5% and negligible for most time frequencies and over most regions, which holds also at the continental scale. Robust positive change signals appear over the south-western and northernmost regions for the variability of the whole daily series (Fig. 4b), and over central-eastern and northern regions for the D2D variability of the series (Fig. 4n). Robust negative signals appear over Iberia for the M2M and D2D variability of the series (Fig. 4k,n).

Finally we investigated how changes could be assuming that the PV and the wind power production series could reach, in the future, a perfect anticorrelation. Under such an ideal theoretical assumption, the variability of the whole daily series of PV-plus-wind power production could be reduced between 5 and 25% (15% at the European level, Fig. 4c), with the D2D variability term holding the best expectations: 5–15% of reduction all over central and southern Europe (Fig. 4o).

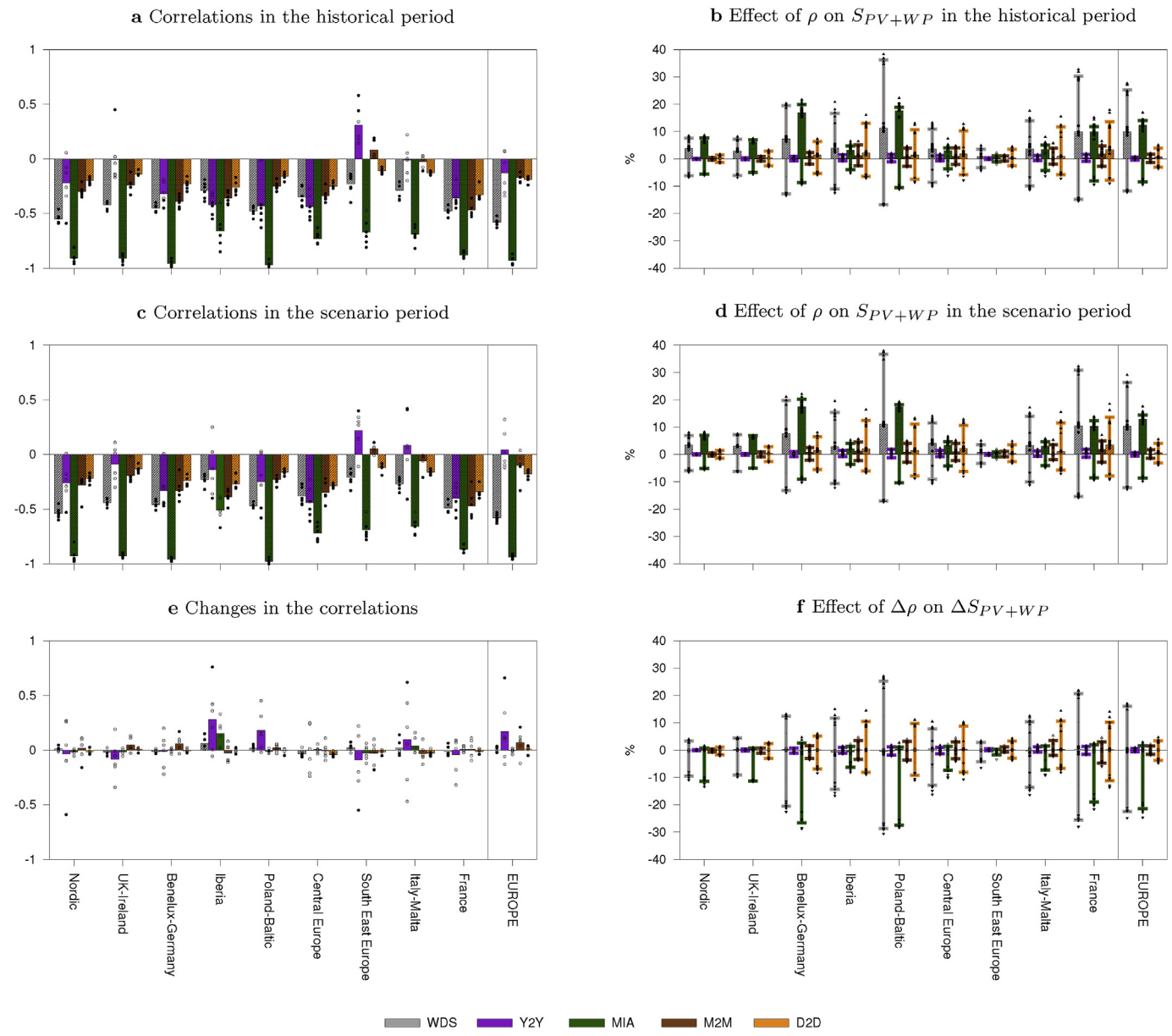

Fig. 3. *Role of (anti)correlation.* Left column: Temporal correlations between the PV and wind power production series under historical (a) and scenario (c) climate conditions at the various temporal frequencies considered in this work (Y2Y, MIA, M2M and D2D) as well as for the whole daily series (WDS). (e) displays the changes in the correlation values between the scenario and the historical period. Color bars represent ensemble mean values. Symbols correspond to each single model/experiment. Black/gray-striped colored bars denote robust/uncertain ensemble mean signals, empty colored bars denote negligible ensemble mean signals, and solid/empty symbols denote significant/non-significant individual signals (see Methods for the followed criteria). Right column: Effect of the temporal correlations between the individual PV and wind power production series on the standard deviation of the joint PV-plus-wind power production series at the various temporal frequencies in the historical (b) and scenario (d) periods (ensemble mean values represented with the colored bars, individual values with circles) along with the upper and bottom limits of such effects for $\rho = -1$ and 1 respectively (the ensemble mean upper-minus-bottom limits range represented by colored range-bars, individual values with triangles for the upper limits and inverted triangles for the bottom limits) according to Eq. (8). Similarly, (f) displays the effect of increased or diminished temporal correlations between the individual production series on the projected changes for the temporal variability of the joint PV-plus-wind production series as well the upper and bottom limits of such effect according to Eq. (11). Black/gray-striped colored bars denote robust/uncertain ensemble mean signals, which, in this case, applies also to the colored range-bars, empty colored bars denote negligible ensemble mean signals, and solid/empty symbols denote significant/non-significant individual signals. Units are dimensionless in panels of the left column and % in panels of the right column.

4. Conclusions and discussion

Previous works have been devoted to assess the spatio-temporal complementarity between wind and solar resources [10–17,28]. Others have paid attention to the climate change impact on either wind or PV power production, individually [20,22,23,29]. However, how their combined response to climate change is, in terms of the temporal variability of the total production, still remained unveiled, at least for Europe.

Here we further demonstrate the temporal complementarity (anticorrelation) of the wind and solar PV production series in their climatological behavior over Europe, which outstands the most because of their typically inverted annual cycles. This holds similarly under both present and future climate conditions. Thus, given that their temporal variability is not projected to undergo important changes individually, small changes in the temporal variability of the combined PV-plus-wind power production are projected: well bellow 5%, negligible for most time frequencies, from daily to

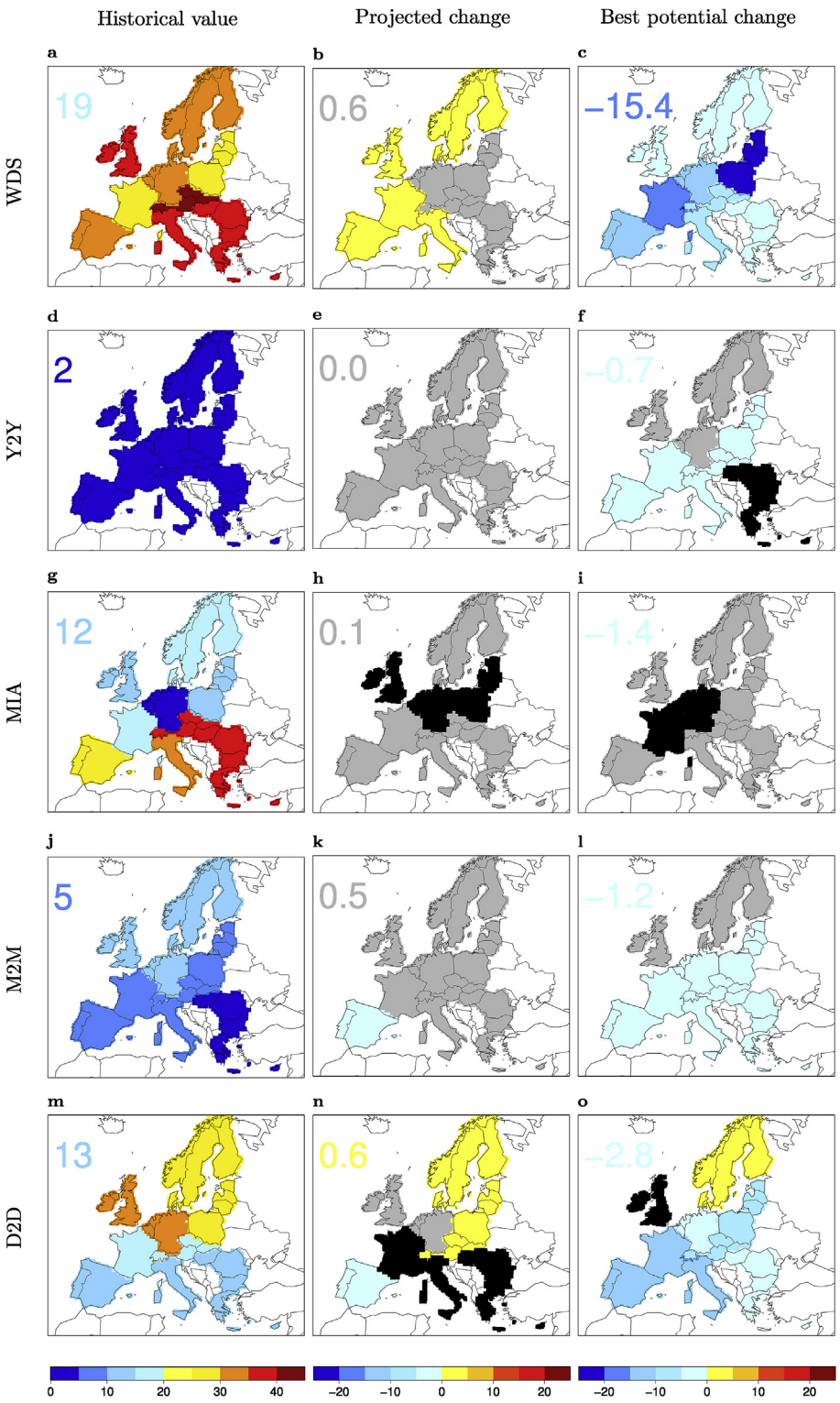

Fig. 4. *Historical values, future projections and best potential changes for the temporal variability of the PV-plus-wind power production.* First column provides the ensemble means of the standard deviation of the whole daily series (first row), and at the various temporal frequencies considered here (Y2Y, MIA, M2M and D2D in second, third, fourth and fifth rows, respectively), of the PV-plus-wind power production (S_{PV+WP}) in the historical period in each region (units: %). Second column provides the ensemble means of the projected changes in S_{PV+WP} (units: %) with black/gray shadows masking the regions where signals are uncertain/negligible. Third column provides the ensemble means of the potential changes in S_{PV+WP} if the correlations between the individual PV and wind power production series reached −1 in the scenario period, i.e. F(-1) following the notation of Section 2.6 (units: %), with black/gray shadows masking the regions where the benefits, as compared to the projections of the second column, are uncertain/negligible. Numbers correspond to the European region as a whole, colored following the same criteria as for the regional shadows.

annual, and over most regions. This implies that the energy background and storage strategies needed to guarantee the supply stability, in a scenario with a high penetration of the variable renewable in the grid, can be designed considering the current climate behavior and will still work under changed climate conditions.

Additionally, we investigated how these changes would be under an ideal future scenario where the individual PV and wind power production series were perfectly anticorrelated in time, while maintained their characteristic mean and standard deviation values (as these magnitudes are, essentially, not projected to change). This scenario drew potential significant reductions in the variability of the daily PV-plus-wind power production series, upper-bounded at 5–25% across regions, 15% at the European level, with the highest benefits rebounding on the high frequency day-to-day variability of the combined production series. These are just upper theoretical bounds, but could motivate smart deployment plans that look for highly complementary locations (holistically) for the new PV and wind power installations, instead of highly rated ones (individually), as this could actually enhance the self-regulation of the stability of the wind-plus-solar power production system.

Alternative approaches for minimizing the variability of the combined production could be based on minimizing the variability of the PV and wind power production series individually, or could investigate how to reach a better balance between them by modifying their regional shares. In any case, while a stable production is clearly a sign of energy security, in practice, the time-varying demand is the driving factor, and production should follow it. Hence future research is needed on the feasibility of the various supply-security approaches, including the energy demand factor, adopting holistic and practical perspectives tailored to the challenges of the energy sector, and taking into account geophysical constraints [30]. Also, efforts should be allocated to improve the regional climate projections in order to enhance the reliability of the climate change impact assessments and narrow the uncertainties around the ensemble mean signals. Currently, regional climate models miss (or may miss) important processes and feedbacks that are likely to have an important fingerprint in the simulation of the renewable potential, such as the aerosol-radiation and aerosol-clouds interactions [31–33] and the radiative effect of the greenhouse gases increase at regional level [34].

Conflicts of interest

The Authors declare no conflict of interests.

Acknowledgments

This study was financially supported by the Fundación Séneca – Regional Agency for Science and Technology of Murcia – through the CLIMAX project (20642/JLI/18), by the Spanish Ministry of Economy and Competitiveness through the projects REPAIR (CGL2014-59677-R) and ACEX (CGL2017-87921-R), also partially funded by the European Regional Development Fund (FEDER), and by the Fundación Biodiversidad of the Spanish Ministry for the Ecological Transition. M. Turco has received funding from the European Union's Horizon 2020 research and innovation programme under the Marie Skłodowska-Curie grant agreement No. 740073 (CLIM4CROP project). S. Jerez has received funding from the *Plan Propio de Investigación* of the University of Murcia (grant No. UMU-2017-10604).

References

[1] Intergovernmental Panel on Climate Change, Climate Change 2014: Mitigation of Climate Change. Contribution of Working Group III to the Fifth Assessment Report of the Intergovernmental Panel on Climate Change, Cambridge Univ. Press, 2015.
[2] M. Höök, X. Tang, Depletion of fossil fuels and anthropogenic climate change — a review, Energy Policy 52 (2013) 797–809.
[3] I. Capellán-Pérez, M. Mediavilla, C. de Castro, Ó. Carpintero, L.J. Miguel, Fossil fuel depletion and socio-economic scenarios: an integrated approach, Energy 77 (2014) 641–666.
[4] N.L. Panwar, S.C. Kaushik, S. Kothari, Role of renewable energy sources in environmental protection: a review, Renew. Sustain. Energy Rev. 15 (3) (2011) 1513–1524.
[5] S. Awerbuch, Portfolio-based electricity generation planning: policy implications for renewables and energy security, Mitig. Adapt. Strategies Glob. Change 11 (3) (2006) 693–710.
[6] F. Sissine, Energy Independence and Security Act of 2007: a Summary of Major Provisions, Library of Congress Washington DC Congressional Research Service, 2007.
[7] European Climate Foundation, Roadmap 2050: a Practical Guide to a Prosperous, Low-Carbon Europe, vol. 1, 2010. Technical and Economic Assessment, www.roadmap2050.eu/project/roadmap-2050.
[8] M.K. Deshmukh, S.S. Deshmukh, Modeling of hybrid renewable energy systems, Renew. Sustain. Energy Rev. 12 (1) (2008) 235–249.
[9] M. Huber, D. Dimkova, T. Hamacher, Integration of wind and solar power in Europe: assessment of flexibility requirements, Energy 69 (2014) 236–246.
[10] F.J. Santos-Alamillos, D. Pozo-Vázquez, J.A. Ruiz-Arias, V. Lara-Fanego, J. Tovar-Pescador, Analysis of spatiotemporal balancing between wind and solar energy resources in the southern Iberian Peninsula, J. Appl. Meteorol. Climatol. 51 (11) (2012) 2005–2024.
[11] F.J. Santos-Alamillos, D. Pozo-Vázquez, J.A. Ruiz-Arias, L. Von Bremen, J. Tovar-Pescador, Combining wind farms with concentrating solar plants to provide stable renewable power, Renew. Energy 76 (2015) 539–550.
[12] S. Jerez, R.M. Trigo, A. Sarsa, R. Lorente-Plazas, D. Pozo-Vázquez, J.P. Montávez, Spatio-temporal complementarity between solar and wind power in the Iberian Peninsula, Energy Proced. 40 (2013) 48–57.
[13] P.E. Bett, H.E. Thornton, The climatological relationships between wind and solar energy supply in Britain, Renew. Energy 87 (2016) 96–110.
[14] N.S. Thomaidis, F.J. Santos-Alamillos, D. Pozo-Vázquez, J. Usaola-García, Optimal management of wind and solar energy resources, Comput. Oper. Res. 66 (2016) 284–291.
[15] C.M. Grams, R. Beerli, S. Pfenninger, I. Staffell, H. Wernli, Balancing Europe's wind-power output through spatial deployment informed by weather regimes, Nat. Clim. Change 7 (8) (2017) 557–562.
[16] M.M. Miglietta, T. Huld, F. Monforti-Ferrario, Local complementarity of wind and solar energy resources over Europe: an assessment study from a meteorological perspective, J. Appl. Meteorol. Climatol. 56 (1) (2017) 217–234.
[17] A.A. Prasad, R.A. Taylor, M. Kay, Assessment of solar and wind resource synergy in Australia, Appl. Energy 190 (2017) 354–367.
[18] S.C. Pryor, R.J. Barthelmie, Climate change impacts on wind energy: a review, Renew. Sustain. Energy Rev. 14 (1) (2010) 430–437.
[19] J.A. Crook, L.A. Jones, P.M. Forster, R. Crook, Climate change impacts on future photovoltaic and concentrated solar power energy output, Energy Environ. Sci. 4 (9) (2011) 3101–3109.
[20] S. Jerez, I. Tobin, R. Vautard, J.P. Montávez, J.M. López-Romero, F. Thais, B. Bartok, O.B. Christensen, A. Colette, M. Déqué, G. Nikulin, The impact of climate change on photovoltaic power generation in Europe, Nat. Commun. 6 (2015) 10014.
[21] M. Reyers, J.G. Pinto, J. Moemken, Statistical–dynamical downscaling for wind energy potentials: evaluation and applications to decadal hindcasts and climate change projections, Int. J. Climatol. 35 (2) (2015) 229–244.
[22] I. Tobin, R. Vautard, I. Balog, F.M. Bréon, S. Jerez, P.M. Ruti, F. Thais, M. Vrac, P. Yiou, Assessing climate change impacts on European wind energy from ENSEMBLES high-resolution climate projections, Clim. Change 128 (1–2) (2015) 99–112.
[23] I. Tobin, S. Jerez, R. Vautard, F. Thais, E. van Meijgaard, A. Prein, M. Déqué, S. Kotlarski, C.F. Maule, G. Nikulin, T. Noël, Climate change impacts on the power generation potential of a European mid-century wind farms scenario, Environ. Res. Lett. 11 (3) (2016), 034013.
[24] J.S. Hosking, D. MacLeod, T. Phillips, C.R. Holmes, P. Watson, E.F. Shuckburgh, D. Mitchell, Changes in European wind energy generation potential within a 1.5° C warmer world, Environ. Res. Lett. 13 (5) (2018), 054032.
[25] I. Tobin, W. Greuell, S. Jerez, F. Ludwig, V. Vautard, M.T.H. van Vliet, F.-M. Bréon, Vulnerabilities and resilience of European power generation to 1.5°C, 2°C and 3°C warming, Environ. Res. Lett. 13 (4) (2018), 044024.
[26] R.H. Moss, J.A. Edmonds, K.A. Hibbard, M.R. Manning, S.K. Rose, D.P. Van Vuuren, T.R. Carter, S. Emori, M. Kainuma, T. Kram, G.A. Meehl, The next generation of scenarios for climate change research and assessment, Nature 463 (7282) (2010) 747.
[27] S. Jerez, F. Thais, I. Tobin, M. Wild, A. Colette, P. Yiou, R. Vautard, The CLIMIX model: a tool to create and evaluate spatially-resolved scenarios of photovoltaic and wind power development, Renew. Sustain. Energy Rev. 42 (2015) 1–15.

[28] S. Jerez, R.M. Trigo, Time-scale and extent at which large-scale circulation modes determine the wind and solar potential in the Iberian Peninsula, Environ. Res. Lett. 8 (4) (2013), 044035.
[29] J. Müller, D. Folini, M. Wild, S. Pfenninger, CMIP-5 models project photovoltaics are a no-regrets investment in Europe irrespective of climate change, Energy 171 (2018) 135–148.
[30] M.R. Shaner, S.J. Davis, N.S. Lewis, K. Caldeira, Geophysical constraints on the reliability of solar and wind power in the United States, Energy Environ. Sci. 11 (4) (2018) 914–925.
[31] P. Nabat, S. Somot, M. Mallet, F. Sevault, M. Chiacchio, M. Wild, Direct and semi-direct aerosol radiative effect on the Mediterranean climate variability using a coupled regional climate system model, Clim. Dyn. 44 (3–4) (2015) 1127–1155.
[32] X. Li, F. Wagner, W. Peng, J. Yang, D.L. Mauzerall, Reduction of Solar Photovoltaic Resources Due to Air Pollution in China, Proceedings of the National Academy of Sciences, 2017, 201711462.
[33] C. Gutiérrez, S. Somot, P. Nabat, M. Mallet, M.Á. Gaertner, O. Perpiñán, Impact of aerosols on the spatiotemporal variability of photovoltaic energy production in the Euro-Mediterranean area, Sol. Energy 174 (2018) 1142–1152.
[34] S. Jerez, J.M. López-Romero, M. Turco, P. Jiménez-Guerrero, R. Vautard, J.P. Montávez, Impact of evolving greenhouse gas forcing on the warming signal in regional climate model experiments, Nat. Commun. 9 (1) (2018) 1304.